Increased risk of groundwater contamination due to saltwater intrusion driven by climate change in Casco Bay, Maine

Matthew Guiang[1], Melissa R. Allen[1*]

1. Oak Ridge National Laboratory, 1 Bethel Valley Rd, Oak Ridge, TN, 37830
   Email: allenmr@ornl.gov

Abstract. Changing precipitation patterns resulting from climate change are likely to affect the future availability of freshwater resources. Coastal aquifers are especially vulnerable to such changes in the form of contamination via the intrusion of saltwater as sea level rises. In Casco Bay, Maine, the population depends largely on groundwater from private wells as a source of freshwater. Thus, assessing the vulnerabilities of coastal and island aquifers to saltwater intrusion influenced by climate change is important. This study examines the aggregate effects of sea level rise, changing precipitation patterns, and population shifts (well pumping rate) on the depth of the freshwater-saltwater interface. Well vulnerability to these changes is determined by comparison of average well depth to the resulting interface depth. Although vulnerabilities of individual wells are difficult to predict given that hydraulic properties are governed by complex fracture patterns, this preliminary model demonstrates a representative response of bedrock aquifers of Casco Bay to climate and population stresses. This study finds that changing precipitation patterns have the greatest effect on interface depth variations, exceeding those caused by sea level rise. Wells near shore where the interface is the shallowest are particularly vulnerable to contamination by saltwater intrusion and should be considered vulnerable even under best-case conditions. In multiple climate change scenarios, the saltwater-freshwater interface decreases in depth, indicating greater vulnerability to contamination over time for populations reliant on groundwater from bedrock aquifer wells.

Keywords: Coastal Aquifers·Climate Change·Salt-water/fresh-water relations·MODFLOW·Maine

1. Introduction

The changing climate has cast into focus the importance of the future availability of freshwater resources (Ferguson and Gleeson 2012; Milly et al. 2005; Vorosmarty et al. 2000). Fluctuating regional populations, coupled with changing weather patterns, alter demand and supply limiting the availability future freshwater resources. In areas such as coastal Maine, where the population is largely dependent upon groundwater extracted from fractured, confined bedrock aquifers, changing precipitation patterns are expected to have significant impacts on the amounts of subsurface freshwater (Caswell 1979). Specifically, sea level rise will alter aquifer hydraulic gradients. Changing rates of precipitation will result in changing rates of aquifer recharge, which will in turn have an effect on the flow of groundwater through aquifer systems. In the area of Casco Bay, Maine (Figure 1), where island and peninsular wells are predominantly drilled into confined bedrock aquifers, these changes become especially important due to networks of fractures that serve as conduits for both freshwater and saltwater to flow into and out of the aquifer. Changes in flow patterns due to rising sea levels and changing rates of recharge can result in the inward flow of saltwater from the sea into the aquifer, effectively contaminating the freshwater resource.

DRAFT

Saltwater intrusion poses a great risk to the residents of coastal Maine due to its relative permanence and difficulty to reverse, especially for communities in which aquifers provide the sole source of drinking water (Tuttle 2007). Coastal areas analogous to Casco Bay have been observed to experience intrusion (Caswell 1979; Tuttle 2007) and are likely to become more vulnerable due to the effects related to climate change. A preliminary analysis of saltwater intrusion risk from sea level rise in Casco Bay, Maine finds that the hydraulic gradient weakens with sea level rise to the point of becoming negative, at which point saltwater flows inward and contaminates the aquifer, demonstrating the vulnerability of these coastal aquifers to saltwater intrusion due to sea level rise. This further analysis uses the United States Geology Survey MODFLOW-2005 program (Harbaugh 2005) to simulate groundwater flow for an example Casco Bay bedrock aquifer and to assess the likelihood of saltwater intrusion of wells under three different influences: 1) sea level rise 2) changing rates of aquifer recharge under the worst case (8.5 W m^{-2} radiative forcing by 2011) Representative Concentration Pathway Scenario (RCP 8.5) precipitation projections, and 3) changing pumping rates due to population shifts.

2. Background

2.1 Confined Bedrock Aquifers

Approximately 40% of Maine's population depends on groundwater for residential use (Caswell 1979). Residents of the islands and peninsulas in Casco Bay rely predominantly on groundwater supplied by wells drilled into fractured, confined bedrock aquifers, the characteristics of which are significant factors affecting the subsurface flow. A map of the private confined bedrock aquifer wells in the Casco Bay area can be seen in Figure 2. A confined aquifer is defined as bedrock overlain by thick permeable soils or pervious bedrock with no soil that is fully saturated with water under pressure (Bobba 1993). Confined bedrock aquifers exist only where rock is fractured and capable of holding water. Flow of groundwater in such aquifers is slow, and its recharge occurs through regular precipitation.

Freshwater in coastal aquifers such as those in Casco Bay, where islands and peninsulas are surrounded by saltwater, exists as a lens that floats above the saltwater in isostatic equilibrium, a schematic of which is shown in Figure 3 (modified from Caswell 1979). The depth of the saltwater-freshwater interface varies seasonally and depends upon climatic conditions, flow within the system, and the extent of groundwater extraction, and is related to the height of the water table elevation by the density ratio of freshwater to saltwater, given by the Ghyben-Herzberg approximation (Herzberg 1901; Ghyben 1889):

$$z=\frac{\rho_f}{\rho_s-\rho_f}h=\alpha h \qquad (1)$$

where $z = z(x)$ is the depth of the freshwater-saltwater interface below mean sea level [m], ρ_f is the fresh water density [kg/L], ρ_s is the saltwater density [kg/L], and $h = h(x)$ is the water table elevation above mean sea level [m] (Werner and Simmons 2009). This ratio is generally considered to be 40:1, meaning that for every meter of freshwater in the aquifer above sea level the lens extends 40 meters below sea level. Correspondingly, for every meter of water drawdown caused by pumping, there is an upwelling of the saltwater-freshwater interface of 40 meters. Due

to this relationship, Ferguson and Gleeson (2012) find that such coastal aquifers are more vulnerable to saltwater intrusion due to groundwater extraction than to predicted sea level rise.

Saltwater intrusion into coastal bedrock aquifers occurs where significant freshwater-bearing fractures, typically associated with faults, intersect large fractures that cut across the land and extend to the ocean (Caswell 1987). These fractures provide saltwater with a path to reach the freshwater stored in bedrock aquifers. Under the conditions of a negative hydraulic gradient, saltwater flows inward from the ocean through these fractures resulting in the migration of the freshwater-saltwater boundary inwards and the consequent contamination of bedrock aquifer wells. It has been shown by Masterson (2004) that for Cape Cod aquifers from years 1921 to 2000, the hydraulic gradient weakens with sea level rise, assuming the water table elevation does not change. In the generalized case study of Werner and Simmons (2009), a similar result was found for head-controlled aquifer systems.

2.2 Geologic Setting

Bedrock in the Harpswell area of Casco Bay consists primarily of metamorphic stratified schistose and granofelsic rocks, predominantly from two geologic formations: the Sebascodegan Formation, a thin-bedded quartz-plagioclase-biotite granofels and gneiss, and the Cape Elizabeth Formation, a thin-bedded siliceous and sericitic slate with beds of greywacke slate and schist (Hussey 1985; Hussey and Marvinney 2002). These geologic units were heavily deformed and metamorphosed at great depths and pressures during the continental collision that formed the Appalachians, resulting in extensive regional faulting and folding, which contributes greatly to the presence of fractures that control groundwater flow in coastal aquifers. Two major oppositely striking thrust faults of moderate dip (~80°) run roughly N-S through Sebascodegan Island, and are coincident with major topographic features and foliation, and are likely related to many of the water bearing fractures in the area (Hussey 1985; Caswell 1979). Sand, gravel, and unconsolidated sediments of varying thickness deposited during the last glacial period cover much of Casco Bay. On Sebascodegan Island the surficial materials are predominantly less than one meter of glacial drift covering bedrock or a thin deposit of poorly sorted till.

3. Methods

In order to quantify the effect of sea level rise on the vulnerability of Casco Bay's island bedrock wells to saltwater intrusion, a model of groundwater flow for a hypothetical representative island aquifer was configured using the modular finite-difference groundwater flow model (MODFLOW) developed by the United States Geological Survey (USGS; McDonald and Harbaugh 1988). This model is the most widely used in the world for simulating groundwater flow and has been validated extensively since its publication in 1988 (US Geological Survey 1997). MODFLOW-2005 models the three-dimensional flow of groundwater of constant density through porous material based on the partial differential equation (Harbaugh 2005)

$$\frac{\delta}{\delta \mathrm{x}}\left(K_{\mathrm{xx}}\frac{\delta h}{\delta \mathrm{x}}\right)+\frac{\delta}{\delta \mathrm{y}}\left(K_{yy}\frac{\delta h}{\delta \mathrm{y}}\right)+\frac{\delta}{\delta \mathrm{y}}\left(K_{\mathrm{zz}}\frac{\delta h}{\delta z}\right)+W=S_s\frac{\delta h}{\delta t} \qquad (2)$$

where K_{xx}, K_{yy}, and K_{zz} are the hydraulic conductivities in the x, y, and z, directions [L/T]; h is the potentiometric head [L]; W is the volumetric flux per unit volume [T^{-1}], S_s is the specific storage of the material [L^{-1}]; and t is time [T]. MODFLOW-2005 uses the finite-difference method to obtain approximate analytical solutions to obtain time-varying head distributions that

can be used to characterize the flow system and to calculate the direction and rate of groundwater flow.

The SWI2 package (Bakker et al. 2013) for MODFLOW was added to simulate seawater intrusion into the aquifer allowing for three-dimensional vertically integrated variable-density groundwater flow analysis. The SWI2 package models variable-density flow in an isotropic aquifer, based on Darcy's law for variable-density flow, which can be written as (Post et al. 2007; Bakker et al. 2013)

$$q_{\mathrm{x}} = -K\frac{\delta h_{\mathrm{f}}}{\delta \mathrm{x}} \qquad q_{\mathrm{y}} = -K\frac{\delta h_{\mathrm{f}}}{\delta \mathrm{y}} \qquad q_{\mathrm{z}} = -K\left(\frac{\delta h_{\mathrm{f}}}{\delta \mathrm{z}} + v\right) \tag{3}$$

where q_{x}, q_{y}, and q_{z} are the specific discharge components in the x, y, and z directions [L/T]; K is the freshwater hydraulic conductivity [L/T]; h_{f} is the freshwater head [L], and v is the dimensionless density [unitless]. The SWI2 package allows for the effects of density differences to be incorporated into MODFLOW-2005, and uses the Dupuit approximation in which an aquifer is vertically discretized into zones of differing densities. Derivations of Eqn (1-2) can be found in Rushton and Redshaw (1979) and Bakker et al. (2013), respectively. This model does not consider variations in viscosity and the effects of dispersion and diffusion. The user interface, ModelMuse Version 3, (Winston 2014) was used as a pre-and post-processing tool for the simulation.

Casco Bay aquifers are represented in MODFLOW using a representative island, Sebascodegan Island. The island includes a specified flux boundary to which a recharge rate is applied. The island aquifer is surrounded by ocean extending offshore along all sides that is represented in MODFLOW by a General Head Boundary (GHB) condition in model layer one with an altitude set to the current sea level, after Bjerklie et al. (2012). To simulate gradual sea level rise, constant heads are increased at yearly intervals at the rate of projected sea level rise.

The model domain is discretized into a finite-difference grid of 101 columns and 120 rows, with cell sizes measuring 75 by 100 m. The upper surface of the model corresponds to the surface elevation provided by elevation contours of Sebascodegan Island. The hypothetical aquifer consists of two layers: a thin unit of unconsolidated gravelly glacial drift overlaying a confined layer of fractured crystalline bedrock that extends to 400 m below sea level. The bottom of the model is defined as a no flow boundary.

The model was designed to simulate the effects of sea level rise on the island's coastal aquifer for the years 2000-2070, incorporating the effects of changing precipitation and recharge rates, as well changing pumping rates associated with population changes. After establishing a steady-state condition, the model was used to simulate hypothetical scenarios of long-term change in sea level and aquifer recharge under Representative Concentration Pathway 8.5 (RCP 8.5), the worst case scenario achieving a climate forcing of 8.5 W m^{-2} by 2100. Two sea level rise scenarios were also considered, which assumed a global sea level rise of one meter and two meters, respectively, over the next century.

A total of 270 years was simulated, using one preliminary stress period of 200 years to establish current, steady-state aquifer conditions, and the following 70 years to simulate aquifer

development under projected changes in sea level and recharge. Storage changes between aquifers were not considered, and all stress periods are steady-state.

3.1. Data Sets

Geologic, hydrologic, climactic, and population data are based on observations and projections for Sebascodegan Island and are presumed to be representative of regional island aquifer conditions. The following data sets are used as those inputs to the model.

3.1.1. Sea Level Rise

Sea level rise estimates are based on those of the National Oceanic and Atmospheric Administration for the United States National Climate Assessment (National Climate Assessment 2014), which indicate a "greater than 90% chance" that global mean sea level will rise at least 0.2 meters and no more than 2.0 meters by 2100.

3.1.2. Precipitation and Recharge

Precipitation data (Appendix Figure 8) used to calculate aquifer rate of recharge (Figure 4) are cumulative monthly values at 4 km resolution from the Weather Research and Forecasting (WRF) model dynamically downscaled from Community Earth System Model, Version 1.0 (CESM1) projections at 1 x 1.25 degree spatial resolution under RCP 8.5. The CESM simulation, output at 3-hourly intervals, is an ensemble member of the Coupled Model Intercomparison Project, Version 5 (CIMP5) (Gao et al. 2012). Recharge is calculated as 7.95% of precipitation (Gerber and Hebson 1996). Base-case and 2050 recharge rates were calculated for the simulation, and intermediate years were interpolated from these data.

3.1.3. LandScan Population Projections and Pumping Rates

The LandScan and LandCast data sets at one kilometer resolution were created using a multi-variable dasymetric modeling approach along with spatial data and imagery analysis technologies to disaggregate census counts within administrative boundaries at the town, county, and state levels (http://web.ornl.gov/sci/landscan/ landscan_documentation.shtml). LandCast 2050 population projections (McKee et al. 2015) incorporate the cohort-component methodology outlined by the U.S. Census along with urbanization/land cover conversion projections. Population from these data sets is then aggregated to the census tract (Appendix Figure 9) to provide proxy communities supplied by individual private wells.

Pumping rates were calculated based on a 51 gallons per capita day (gpcd) estimate of Maine public water usage presented by Kenny et al. (2009) and multiplied by projected populations for Sebascodegan Island for 2004 and 2050. Since the vast majority of pumping in the region is from private bedrock wells (Caswell 1979), this is an appropriate estimate. Wells were simulated using the WEL package in MODFLOW, pumping at a depth of 60 m, an average depth of bedrock wells in the region (Caswell 1979; Loiselle and Evans 1995).

3.1.4. Hydraulic Properties and Boundary Conditions

Aquifer properties, (Appendix Table 2), were assigned based on previously measured data and generalized surficial and bedrock geology of the Casco Bay area. The unit comprising layer one is separated into two units (Appendix Figure 7B): fine-grained glaciomoraine deposits (Presumpscot Formation) and glacial till. Surficial materials have various thicknesses

interpolated from the overburden thickness of island wells. Horizontal hydraulic conductivity for the Presumpscot Formation and glacial till is 0.00189 and 1.122 m/d, respectively (Brainerd et al. 1996; Morrissey (1983). Vertical Hydraulic conductivity of the Presumpscot Formation is 8.23×10^{-6} m/d (Nielsen et al. 1995).

Model layer two represents heterogeneous anisotropic crystalline fractured metamorphic bedrock where hydraulic conductivity can vary over at least six orders of magnitude (Johnson 1999). However, Shapiro (2002) shows that at large enough scales, bulk bedrock aquifer properties may be used to infer regional distributions of groundwater. While complex fracture networks govern hydraulic conductivity at small scales, on scales larger than 100 m the effective hydraulic conductivity of the bedrock is more strongly controlled by the larger fracture network and bulk hydraulic properties. Furthermore, Loiselle and Evans (1995) find that in the region of study, fracture permeability remains uniform with depth, validating the use of bulk hydraulic properties for a large-scale model. Thus, layer two is modeled as a homogeneous isotropic layer with a hydraulic conductivity of 0.277 m/d, based on a range of estimates made by Johnson (1999) on similar fractured bedrock. No hydrogeological data was available for the specific bedrock units considered in this study.

As a result of these generalizations, this model must be considered preliminary and requires further, site-specific hydrogeological studies to better constrain the findings of this study. Further, the complex nature and spatial heterogeneity of hydraulic properties of fractured bedrock aquifers limits the ability of this model to predict vulnerability of wells on an individual scale. Rather, this model serves primarily to predict aquifer lens depth at a larger scale and its response to changes relating to climate and population shifts.

4. Results and Discussion

Ten scenarios, shown in Table 1, were simulated using the model. These included a “best” and “worst” case scenario, in order to demonstrate the potential range of responses for the aquifer. The simplest three scenarios demonstrate the individual effects of zero, one, and two meters sea level rise with pumping and recharge rates held constant. An additional three scenarios incorporate projected changes in recharge and pumping rates with the assumed zero, one, and two meters sea level rise. The final two scenarios consider high and low rates of recharge, with sea level constant at current sea level and pumping absent. After each simulation, the depth of the saltwater-freshwater interface was compared to the average well depth (60 m) to determine saltwater contamination vulnerability. Where the interface depth is shallower than the average well depth, that well location is considered vulnerable to saltwater intrusion.

Figure 5 shows the depths of the saltwater-freshwater interface for a cross section of the island under multiple scenarios. In a best case scenario (Figure 5B) assuming no sea level rise, highest-possible recharge rate, and lowest-possible pumping rate, the depth of the interface is up to 21 m deeper than the worst case scenario that assumes two meters sea level rise by 2100, lowest possible recharge rate, and highest possible pumping rate. Figure 5C shows the projected interface depths for a cross section of the island based on projected changes in recharge and pumping rates under three possible sea level rise scenarios (zero, one, and two meters by 2100). The effect of sea level rise can be seen as the depth of the lens decreases by as much as 14 m between zero and two meters sea level rise scenarios.

DRAFT

In scenarios 3-4 and 8-10, which examine the individual effects of sea level rise and recharge, respectively, this study finds that recharge rate has a more significant effect on interface depth than that of projected sea level rise. Also, while pumping does have an effect on the depth of the interface, the rate of pumping occurring at private wells is only enough to cause minor upwellings in the interface. Such an upwelling can be seen in Figure 5C. Thus, over-pumping at private wells is not likely to be a leading contributor to saltwater intrusion, compared to other coastal regions where over-pumping from groundwater wells is the primary cause of saltwater intrusion (Barlow and Reichard 2010).

To determine the vulnerability of individual wells given changes in the saltwater-freshwater interface of the model Sebascodegan Island, geospatially located model wells (Figure 6) of representative depth were used in the simulation. In the best case scenario (Figure 6A), 13 of the 168 total model wells were below the saltwater-freshwater interface (contaminated), assuming an average well depth of 60 m. In the worst case scenario (Figure 6B), the number of contaminated wells was 19. In the climate projection assuming zero meters sea level rise (Figure 6C), 14 wells were contaminated. In the climate projection assuming two meters sea level rise (Figure 6D), 15 wells were contaminated.

This study finds that wells close to shore, where the interface is shallowest, are particularly vulnerable to contamination by saltwater intrusion and should be considered vulnerable even under best-case conditions. With increasingly severe climate change scenarios, the overall depth of the interface decreases, increasing the likelihood of saltwater intrusion into wells. In possible climate change scenarios 5-7 the saltwater-freshwater interface decreases in depth, indicating increased vulnerability to contamination over time for populations reliant on groundwater from bedrock wells. Although individual well vulnerability is difficult to predict given hydraulic properties are governed by complex fracture patterns, this preliminary model is useful in demonstrating the response of bedrock aquifers to climate and population stresses.

It must be stressed that results of this preliminary model demonstrate the only the generalized qualitative response of a coastal bedrock aquifer in Casco Bay to population shifts and the precipitation and sea level changes accompanying climate change. The heterogeneous and complex nature of the bedrock in question can contribute to hydraulic properties varying over many orders of magnitude, variations that can significantly impact models of this kind. In order to better constrain modeling parameters and thus gain more detailed information regarding the vulnerability of specific aquifers, site-specific hydrogeologic data is needed for the bedrock and surficial materials in the region. Improving and localizing estimates of hydraulic properties will serve to paint a more accurate picture of the vulnerability of these aquifers.

5. Conclusions

This study finds that climate change projections indicate increased annual precipitation (although mostly in the form of larger extreme events) for the islands in the Casco Bay area. Coupled with a projected decrease in population, and therefore a decrease in private pumping rates, this change seems unlikely to put freshwater wells drawing from confined bedrock aquifers at risk. However, the effects of sea level rise could serve to decrease the depth of the interface to the point at which risk is increased for some wells. Thus, although mitigated by a projected increase in precipitation

amounts for the northeast, a rise in sea level causes significant shallowing of the saltwater-freshwater interface, and the sum total of the effects climate change could contribute to the possible contamination of some private wells. While individual well vulnerability is difficult to predict given the complex and heterogeneous nature of fractured bedrock, deep wells that are close to shore are most at risk for contamination, and should be considered especially vulnerable to this long term consequence of climate change.

Acknowledgements

This manuscript has been authored by employees of UT-Battelle, LLC, under contract DE-AC05-00OR22725 with the U.S. Department of Energy. Accordingly, the publisher, by accepting the article for publication, acknowledges that the United States Government retains a nonexclusive, paid-up, irrevocable, world-wide license to publish or reproduce the published form of this manuscript, or allow others to do so, for United States Government purposes.

The authors would like to acknowledge the financial support for this research from the United States Department of Homeland Security (DHS) Regional Resiliency Assessment Program (RRAP) and from the U. S. Department of Energy Office of Science (DOESC) and the Oak Ridge Institute for Science and Education (ORISE) Science Undergraduate Laboratory Internships (SULI) at Oak Ridge National Laboratory. We also gratefully acknowledge the intellectual and data contributions of DHS's Donald Kim Erskine, IP Regional Director, Federal Region 1 and William DeLong, PSA Maine District; Duane Verner, Risk and Infrastructure Science Center (RISC), Global Security Sciences Division, Argonne National Laboratory; Robert Marvinney, Maine State Geologist; and Steven Fernandez, Civil and Environmental Engineering, University of Tennessee.

References

Bakker M, Schaars F, Hughes JD, Langevin CD, Dausman AM (2013) Documentation of the seawater intrusion (SWI2) package for MODFLOW. Book 6, Chap A46:1-47, US Geol Surv Techs and Methods

Barlow PM, Reichard EG (2010) Saltwater intrusion in coastal regions of North America, Hydrogeology J. 18(1):247-260, doi 10.1007/s10040-009-0514-3

Bjerklie DM, Mullaney JR, Stone JR, Skinner BJ, Ramlow, MA (2012) Preliminary investigation of the effects of sea-level rise on groundwater levels in New Haven, Connecticut. US Geol Surv Open-File Rep 2012-1025

Bobba AG (1993) Mathematical model for saltwater intrusion in coastal aquifers, Water Resources Management. 7(1):3-37, doi 10.1007/BF00872240

Brainerd EC, Hebson CS, Gerber RG (1996) Hydrogeology of Presumpscot clay-silt using isotopes. In: Loiselle M, Weddle TK, White C (eds) Selected papers on the hydrogeology of Maine. Bulletin 4, Geol Soc Maine, Augusta, Maine

Caswell WB (1979) Maine's ground-water situation, Ground Water. 17(3):235-243, doi 10.1111/j.1745-6584.1979.tb03317.x

Caswell WB (1987) Ground water handbook for the state of Maine. Bulletin 39, Maine Geol Surv, Augusta, ME

Ghyben BW (1889) Nota in Verband met de Voorgenomen Putboring Nabij Amsterdam [Note concerning planned well drilling near Amsterdam]. Tijdschr Kon Inst Ing, 1888-1889:8–22,

Ferguson G, Gleeson T (2012) Vulnerability of coastal aquifers to groundwater use and climate change, Nature Climate Change. 2:342-345, doi 10.1038/nclimate1413

Gao Y, Fu JS, Drake JB, Liu Y, Lamarque, JF (2012) Projected changes of extreme weather events in the eastern United States based on a high resolution climate modeling system, Environ. Res. Lett. 7(4):044025, doi 10.1088/1748-9326/7/4/044025

Gerber RG, Hebson CS (1996) Ground water recharge rates for Maine soils and Bedrock. In: Loiselle M (ed) Selected papers on the hydrogeology of Maine. Geol Soc Maine, p 23-52

Harbaugh AW (2005) MODFLOW-2005: The US Geological Survey modular ground-water model -- the Ground-Water Flow Process. US Geol Surv Techniques and Methods 6-A16

Herzberg A (1901) Die Wasserversorgung einiger Nordseebäder [The water supply of some North Sea Sites]. J Gasbeleucht Wasserversorg 44(44-45):815–844

Hussey AM II (1985) The bedrock geology of the Bath and Portland 2° map sheets, Maine. Maine Geol Surv Open-File 85-87

Hussey AM II, Marvinney RG (2002) Bedrock geology of the Bath 1:100,000 quadrangle. Maine Geol Surv Geologic Map 02-152

Johnson CD (1999) Effects of lithology and fracture characteristics on hydraulic properties in crystalline rock: Mirror Lake Research Site, Grafton County, New Hampshire. In: Morganwalp, DW, Buxton HT (eds) US Geol Surv Toxic Substances Hydrology Program. Proceedings of the Technical Meeting, Charleston, South Carolina, March 1999

Kenny JF, Barber NL, Hutson SS, Linsey KS, Lovelace JK, Maupin MA (2009) Estimated use of water in the United States in 2005. US Geol Surv Circ 1344

Loiselle M, Evans D (1995) Fracture density distributions and well yields in Coastal Maine, Ground Water. 33(2):190-196, doi 10.1111/j.1745-6584.1995.tb00273.x

Lombard PJ (2015) Maine StreamStats: a water-resources web application. US Geol Surv Fact Sheet 2015-3014, doi 10.3133/fs20153014

Masterson JP (2004) Simulated interaction between freshwater and saltwater and effects of groundwater pumping and sea-level change, Lower Cape Cod aquifer system, Massachusetts. US

DRAFT

Geol Surv Sci Invest Rep 2004-5014

McDonald MG, Harbaugh AW (1998) A modular three-dimensional finite-difference ground-water flow model. Book 6, Chapter A1, US Geol Surv Techs Water-Resour Invest

McKee JJ, Rose AN, Bright E, Huynh T, Bhaduri B (2015) A locally-adaptive, spatially-explicit projection of US Population for 2030 and 2050, Proceedings of the National Academy of Sciences, 112(5):1344-1349, doi 10.1073/pnas.1405713112

Milly PCD, Dunne KA, Vecchia AV (2005) Global pattern of trends in streamflow and water availability in a changing climate, Nature. 438:347–350, doi 10.1038/nature04312

Morrissey DJ (1983) Hydrology of the Little Androscoggin River Valley Aquifer, Oxford County, Maine. US Geol Surv Water-Resour Invest, 83-4018

National Climate Assessment (2014) Climate Change Impacts in the United States. http://nca2014.globalchange.gov/report. Cited 21 July 2015

Nielsen MG, Stone JR, Hansen BP, Nielsen JP (1995) Geohydrology, water quality, and conceptual model of the hydrologic system, Saco Landfill area, Saco, Maine. US Geol Surv Water-Resour Invest Rep 95-4027

Post V, Kooi H, Simmons C (2007) Using hydraulic head measurements in variable –density ground water flow analyses, Ground Water. 45(6):664-671, doi 10.1111/j.1745-6584.2007.00339.x

Rushton KR, Redshaw SC (1979) Seepage and groundwater flow: numerical analysis by analog and digital methods. Wiley

Shapiro AM (2002) Characterizing fractured rock for water supply: From well field to the water-shed, Fractured-Rock Aquifers. Proceedings National Ground Water Association, Denver, Colorado, 6-9 2002

Tolman SS (compiler) (2010a) Bedrock well depths in the Bath 30x60-minute quadrangle, Maine. Maine Geol Surv Open-File Map 10-34

Tolman, SS (compiler) (2010b) Overburden thickness in the Bath 30x60-minute quadrangle, Maine. Maine Geol Surv Open-File Map 10-35

Tuttle S (2007) Water Resources of Part of the West Coast of Vinalhaven Island, Penobscot Bay. http://keckgeology.org/files/pdf/symvol/20th/mainewater/tuttle.pdf. Cited 10 Jun 2015.

US Geological Survey (1997) Modeling ground-water flow with MODFLOW and related programs. US Geol Surv Fact Sheet 121-97

Vorosmarty CJ, Green P, Salisbury J, Lammers RB (2000) Global water resources: Vulnerability from climate change and population growth, Science. 289(5477):284–288,

DRAFT

doi 10.1126/science.289.5477.284

Werner AD, Simmons CT (2009) Impact of Sea Level Rise on Sea Water Intrusion in Coastal Aquifers, Ground Water. 47(2):197-204, doi 10.1111/j.1745-6584.2008.00535.x

Winston RB (2009) ModelMuse - A graphical user interface for MODFLOW–2005 and PHAST. US Geol Surv Techniques and Methods 6–A29

DRAFT

Figures

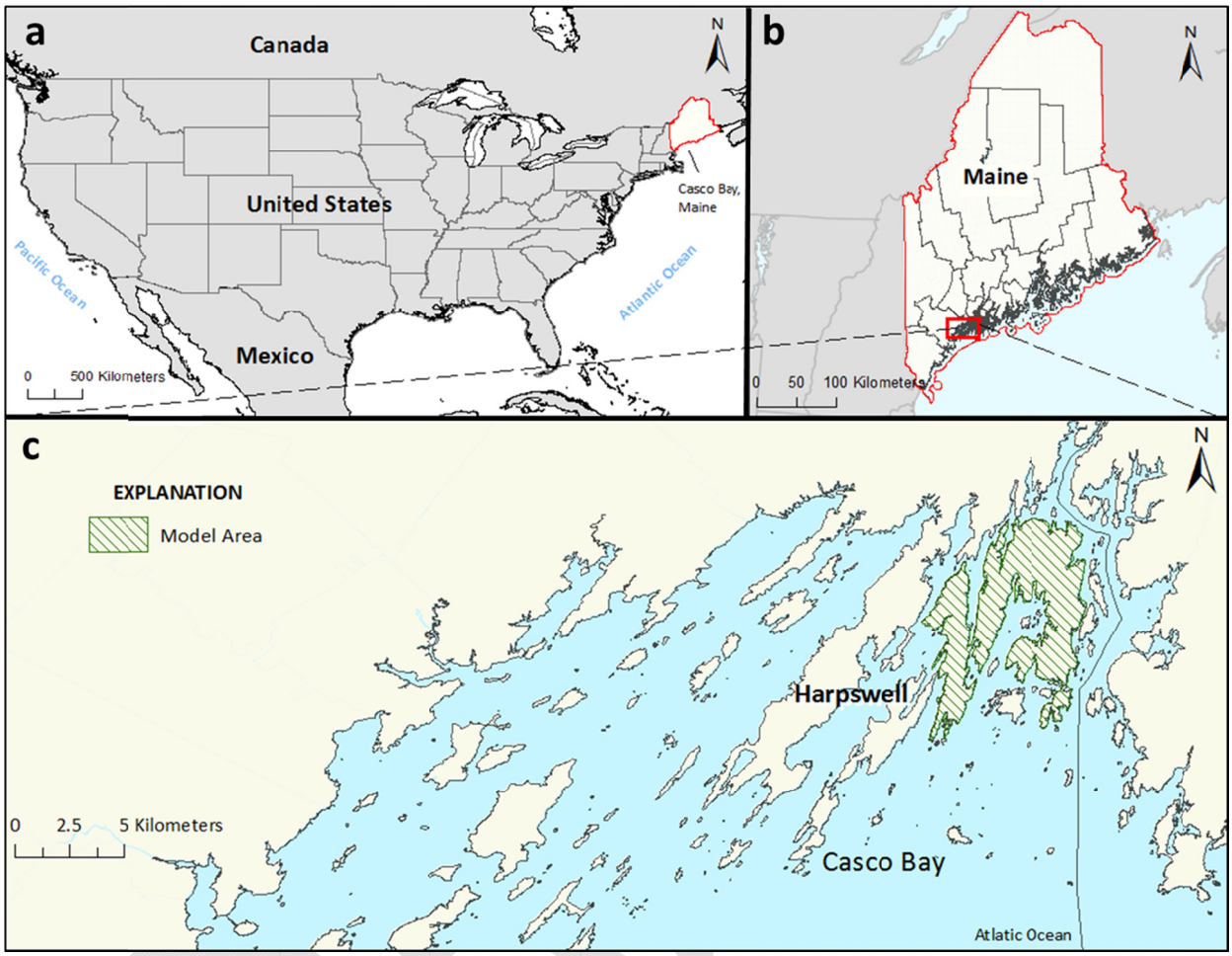

Fig. 1 (a) Map of study area with Maine outlined in *red* and Casco Bay region labeled. **(b)** Focused view of Maine (highlighted by *red line*) with Casco Bay **(1c)** outlined by *red box*. **(c)** Map of Casco Bay region of study with model area represented by the *shaded region*.

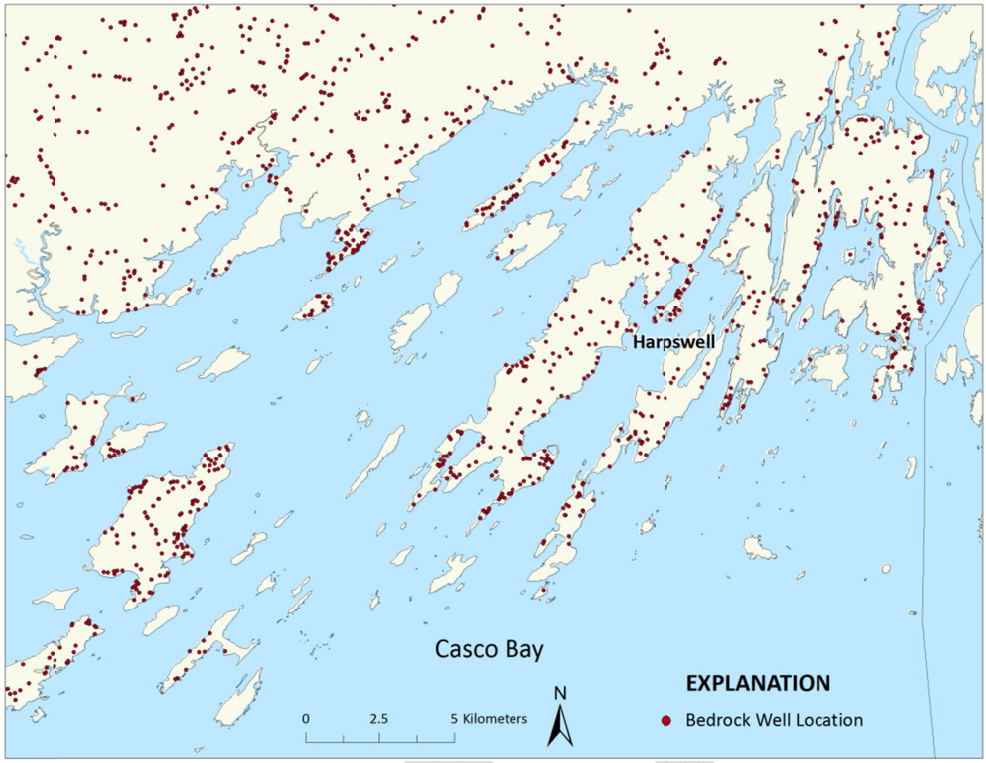

Fig. 2 Map of Casco Bay showing locations of private bedrock well locations (*red circles*) (Tolman, 2010a)

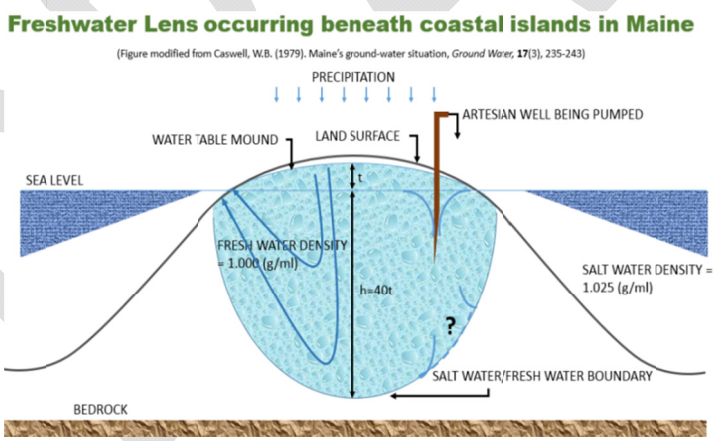

Fig 3 Schematic (modified from Caswell, 1979) showing the idealized geometry of the freshwater lens which floats above the surrounding salt water. The depth of the lens (*h*) is based on saltwater-freshwater density ratio and approximately equal to 40*t*.

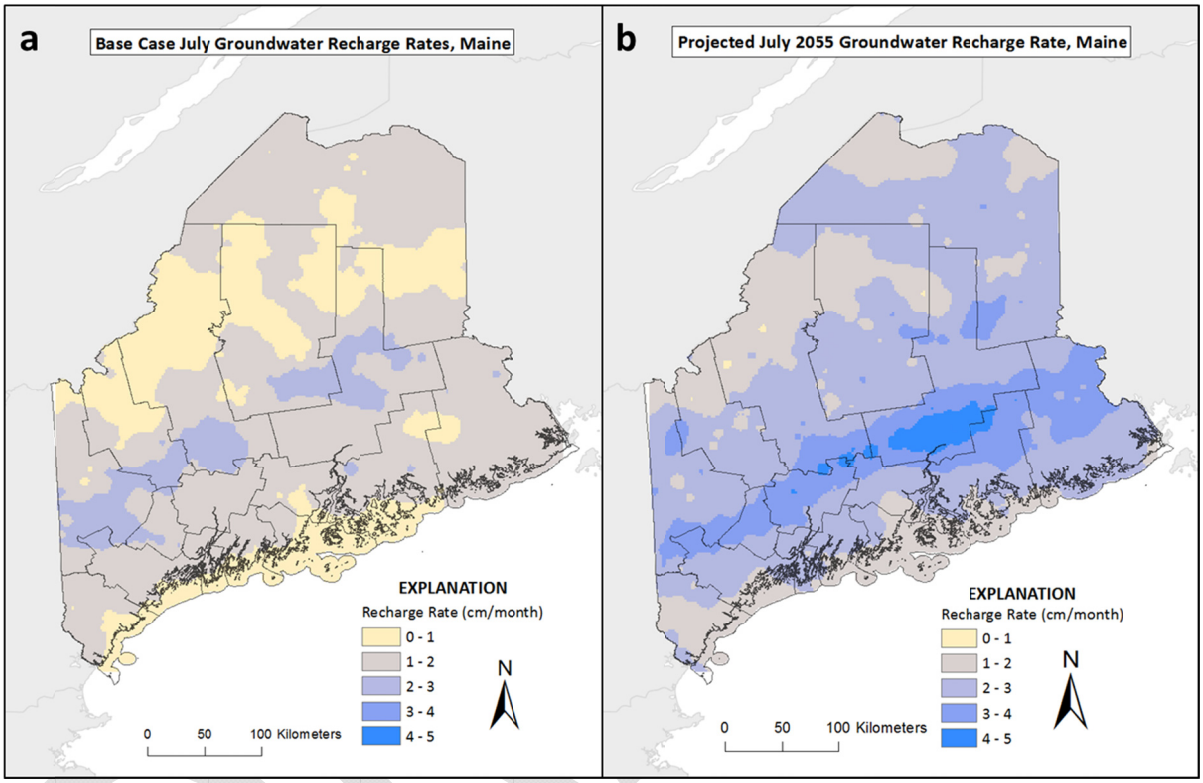

Fig 4 Map showing July **(a)** projected base-case and **(b)** 2055 recharge rates. Recharge rates are calculated as 7.95% of precipitation (projected using WRF dynamically downscaled data) (Gerber and Hebson, 1996). Base-case and 2050 recharge rates were calculated for the simulation, and intermediate years were interpolated from these data.

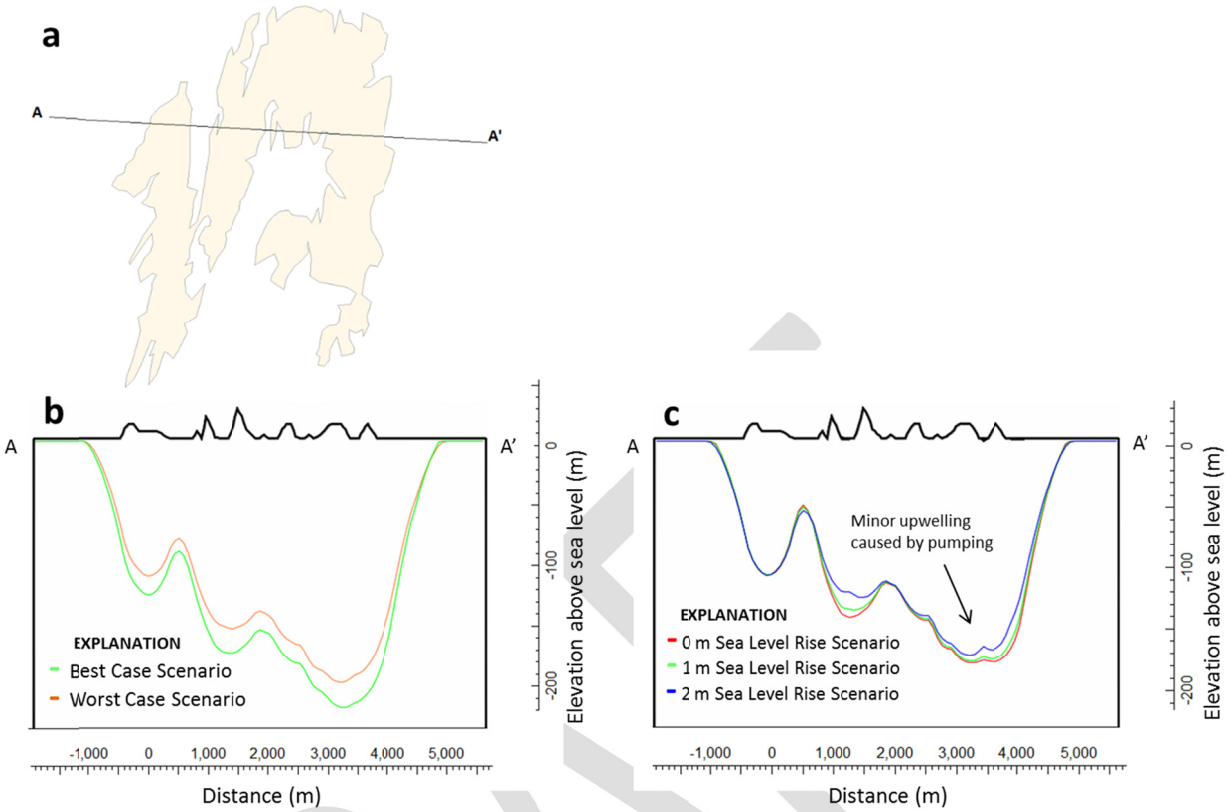

Fig. 5 (a) Map of model area showing cross section A-A'. **(b)** Plot of saltwater-freshwater interface depth (m) for a best case scenario (*green*) assuming no sea level rise, highest-possible recharge rate, and lowest-possible pumping rate, and worst case scenario (*orange*) that assumes two meters sea level rise by 2100, lowest-possible recharge rate, and highest-possible pumping rate. The depth of the worst case interface is up to 21 m shallower than the best case interface. **(c)** Plot of saltwater-freshwater interface depth for climate change projection scenarios considering zero meters (*red*), one meter (*green*) and two meters (*blue*) sea level rise. The depth of the interface can be seen to be decreasing by as much as 14 m under increased sea level rise. The minor upwelling caused by private well pumping is indicated by the *arrow*.

Fig. 6 Map showing model wells and contaminated wells (*colored circles*) in 2070 assuming an average well depth of 60 m, based on **(a)** best case, **(b)** worst case, **(c)** zero meters sea level rise, and **(d)** two meters sea level rise scenarios. In the best case scenario **(a)**, 13 of the total 168 model wells is below the saltwater-freshwater interface (contaminated). In the worst case scenario **(b)**, the number of contaminated wells is 19. In the climate projection assuming zero meters sea level rise **(c)**, 14 wells are contaminated. In the climate projection assuming two meters sea level rise **(d)**, 15 wells are contaminated.

Table 1 Model Scenarios

No.	Scenario	Sea Level Start (m)	Sea Level End (m)	Recharge Start (m/d)	Recharge Start (m/d)	Pumping Rate Start (m^3/d)	Pumping Rate End (m^3/d)
1	Worst Case	2	2	0.000282795	0.000282795	-3.175	-3.175
2	Best Case	0	0	0.000356452	0.000356452	-2.75	-2.75
3	High Recharge	0	0	0.000282795	0.000282785	0	0
4	Low Recharge	0	0	0.000356452	0.000356452	0	0
5	Projection 1 (2 m sea level rise)	0	2	0.000282795	0.000356452	-3.175	-2.75
6	Projection 2 (1 m sea level rise)	0	1	0.000282795	0.000356452	-3.175	-2.75
7	Projection 3 (0 m sea level rise)	0	0	0.000282795	0.000356452	-3.175	-2.75
8	0 m Sea Level Rise	0	0	0.000282795	0.000282795	-3.175	-3.175
9	1 m Sea Level Rise	0	1	0.000282795	0.000282795	-3.175	-3.175
10	2 m Sea Level Rise	0	2	0.000282795	0.000282795	-3.175	-3.175

DRAFT

Appendix 1. Supplementary Material

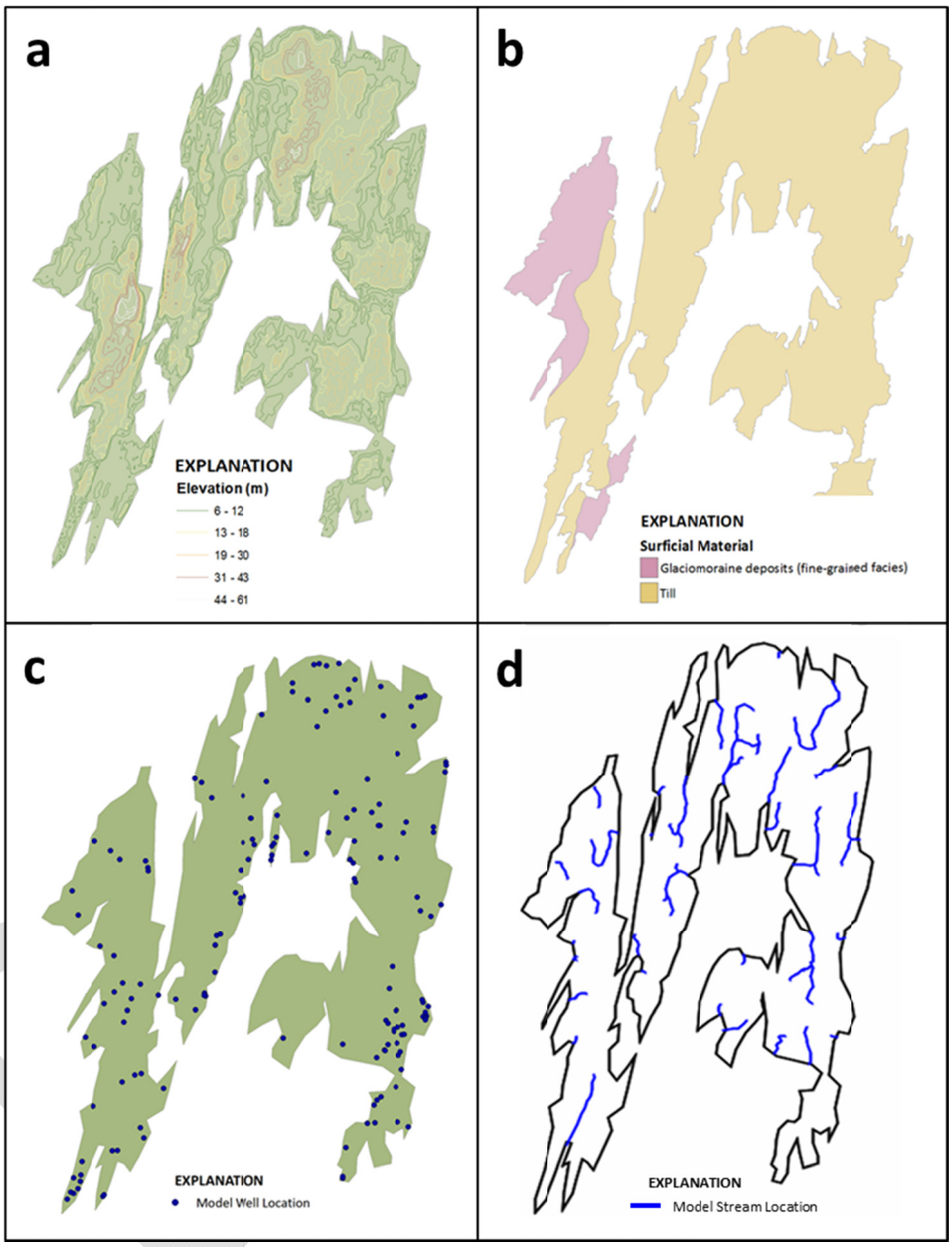

Fig. 7 (a) Elevation contours of Sebascodegan Island interpolated to create model surface elevation. **(b)** Surficial material of Sebascodegan Island. Surficial materials consist of fine-grained glaciomoraine deposits (Presumpscot Formation) and glacial till. The depth of these materials is interpolated based on overburden depth provided by well log data (Tolman, 2010b). **(c)** Model well locations (*blue circles*) for Sebascodegan Island (Tolman, 2010a). Well depth is modeled at 60 m, the average well depth for wells on Sebascodegan Island. **(d)** Model stream locations (*blue lines*) based on those provided by the USGS StreamStats application (Lombard, 2015).

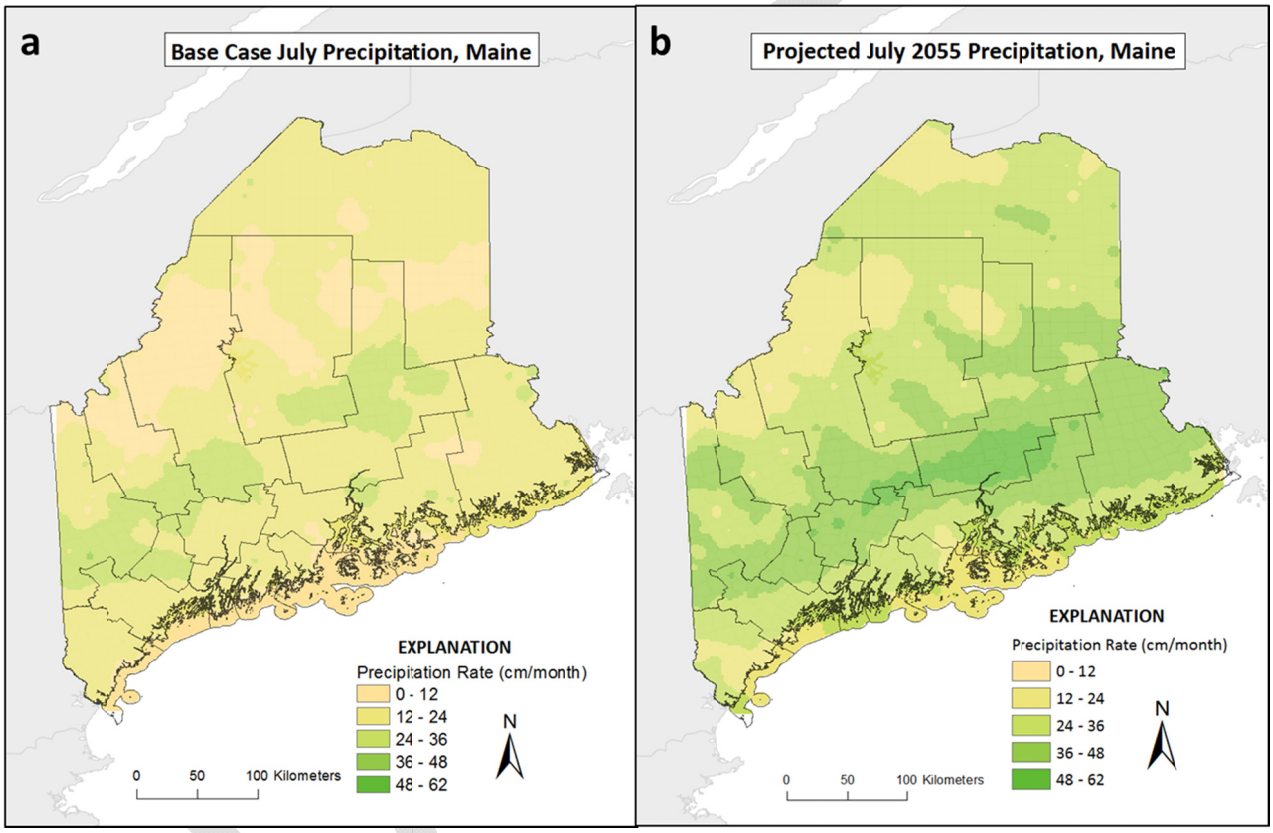

Fig. 8 July projected **(a)** base case and **(b)** 2055 precipitation rates, based on WRF data dynamically downscaled from Community Earth System Model, Version 1.0 (CESM1) projections at 1 x 1.25 degree spatial resolution under RCP 8.5. The CESM simulation, output at 3-hourly intervals, is an ensemble member of the Coupled Model Intercomparison Project, Version 5 (CIMP5) (Gao et al., 2012). Base-case and 2050 precipitation rates were calculated for the simulation, and intermediate years were interpolated from these data.

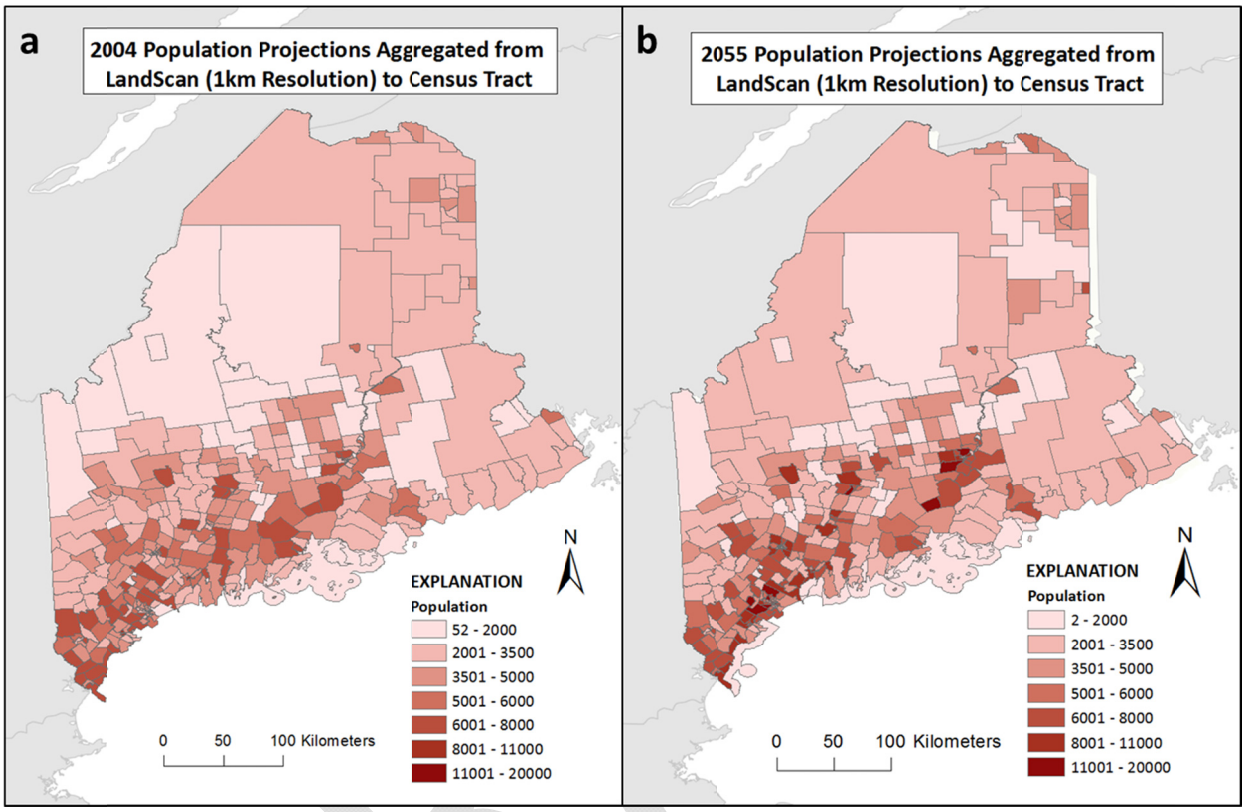

Fig. 9 2004 base case **(a)** and 2055 **(b)** population projections aggregated from LandScan (1 km resolution) to census tract. Population projections for Sebascodegan Island for 2004 are 2,763 and 1,893, respectively. Multiplying these populations by the gallons per capita day (gpcd) private well water use estimates provided by Kenny et al. (2009) gives the total pumping rate per day.

Table 2 Hydraulic Properties of Aquifer Materials

Geologic Material	Layer	Horizontal Hydraulic Conductivity (K_x, m/day)	Vertical Hydraulic Conductivity (K_z, m/day)	Source
Presumpscot Formation	1	0.001889	$8.23*10^{-6*}$	Brainerd et al., 1996; *Nielsen et al., 1995
Till	1	1.121	1.21	Morrissey, 1983
Fractured Metamorphic Crystalline Bedrock	2	0.277	0.277	Johnson, 1999

DRAFT